

BASAL CAMBRIAN DYNAMIC CAPACITY ESTIMATION COMPLETED

Plains CO₂ Reduction (PCOR) Partnership Phase III Task 16 – Milestone M35

Prepared for:

Andrea T. McNemar

National Energy Technology Laboratory
U.S. Department of Energy
3610 Collins Ferry Road
PO Box 880
Morgantown, WV 26507-0880

DOE Cooperative Agreement No. DE-FC26-05NT42592

Prepared by:

Guoxiang Liu
Wesley D. Peck
Charles D. Gorecki
Edward N. Steadman
John A. Harju

Energy & Environmental Research Center
University of North Dakota
15 North 23rd Street, Stop 9018
Grand Forks, ND 58202-9018

EERC DISCLAIMER

LEGAL NOTICE This research report was prepared by the Energy & Environmental Research Center (EERC), an agency of the University of North Dakota, as an account of work sponsored by the U.S. Department of Energy (DOE) National Energy Technology Laboratory (NETL). Because of the research nature of the work performed, neither the EERC nor any of its employees makes any warranty, express or implied, or assumes any legal liability or responsibility for the accuracy, completeness, or usefulness of any information, apparatus, product, or process disclosed or represents that its use would not infringe privately owned rights. Reference herein to any specific commercial product, process, or service by trade name, trademark, manufacturer, or otherwise does not necessarily constitute or imply its endorsement or recommendation by the EERC.

ACKNOWLEDGMENT

This material is based upon work supported by DOE NETL under Award No. DE-FC26-05NT42592.

DOE DISCLAIMER

This report was prepared as an account of work sponsored by an agency of the United States Government. Neither the United States Government, nor any agency thereof, nor any of their employees, makes any warranty, express or implied, or assumes any legal liability or responsibility for the accuracy, completeness, or usefulness of any information, apparatus, product, or process disclosed, or represents that its use would not infringe privately owned rights. Reference herein to any specific commercial product, process, or service by trade name, trademark, manufacturer, or otherwise does not necessarily constitute or imply its endorsement, recommendation, or favoring by the United States Government or any agency thereof. The views and opinions of authors expressed herein do not necessarily state or reflect those of the United States Government or any agency thereof.

NDIC DISCLAIMER

This report was prepared by the EERC pursuant to an agreement partially funded by the Industrial Commission of North Dakota, and neither the EERC nor any of its subcontractors nor the North Dakota Industrial Commission (NDIC) nor any person acting on behalf of either:

- (A) Makes any warranty or representation, express or implied, with respect to the accuracy, completeness, or usefulness of the information contained in this report or that the use of any information, apparatus, method, or process disclosed in this report may not infringe privately owned rights; or

- (B) Assumes any liabilities with respect to the use of, or for damages resulting from the use of, any information, apparatus, method, or process disclosed in this report.

Reference herein to any specific commercial product, process, or service by trade name, trademark, manufacturer, or otherwise does not necessarily constitute or imply its endorsement, recommendation, or favoring by the North Dakota Industrial Commission. The views and opinions of authors expressed herein do not necessarily state or reflect those of the North Dakota Industrial Commission.

TABLE OF CONTENTS

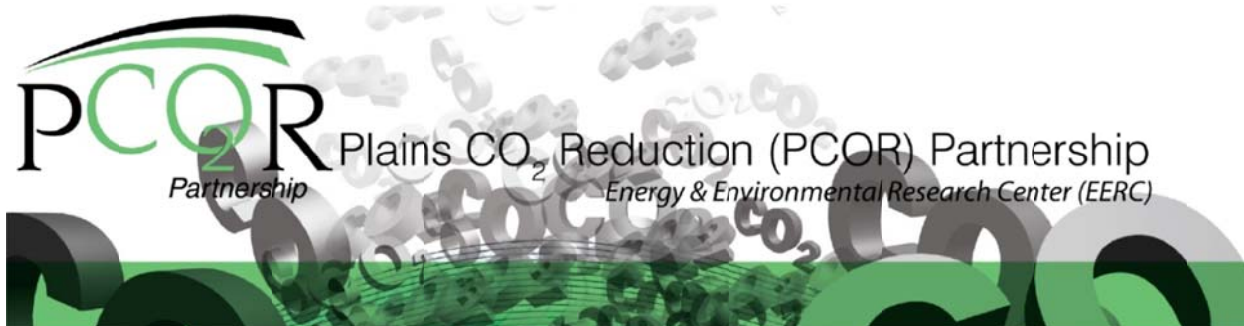
LIST OF FIGURES	i
LIST OF TABLES	i
INTRODUCTION	1
EXPERIMENTAL, RESULTS, AND DISCUSSION	1
CONCLUSIONS.....	7

LIST OF FIGURES

1	Global grid size $35,000 \times 35,000$ ft with local grid refinements in size of 7000×7000 ft marked by polygons overlain on the reservoir permeability	2
2	Location of the 16 CO ₂ sources in the study area (left) and 16 injectors in the simulation model based on the location shown on the left (right)	3
3	210 injectors distributed among the 16 CO ₂ resources	4
4	20 water extractors embedded around the injectors at Duffield Warburg	4
5	Total injected CO ₂ with a time-stepped injection rate for Cases 1–5	5
6	Injection rates for Cases 6 and 7	6
7	Total injected CO ₂ for Cases 6 and 7	6
8	Case 6 pressure differences after 50-year injection (left) and after 36-year postinjection (right)	7
9	Case 7 pressure differences after 50-year injection (left) and after 36-year postinjection (right)	7

LIST OF TABLES

1	Sixteen CO ₂ Sources in the Study Area	2
2	Eight Simulation Scenarios and Results.....	3



BASAL CAMBRIAN DYNAMIC CAPACITY ESTIMATION COMPLETED

INTRODUCTION

As one of the U.S. Department of Energy's Regional Carbon Sequestration Partnerships, the Plains CO₂ Reduction (PCOR) Partnership at the Energy & Environmental Research Center (EERC) is performing a case study on the feasibility of large-scale underground CO₂ storage in the basal saline system of central North America. The area of investigation encompasses approximately 1,500,000 km² of the Alberta and Williston Basins located in the provinces of Alberta, Saskatchewan, and Manitoba in Canada and the states of Montana, North Dakota, and South Dakota in the United States. The thickness of the system is up to 300 m, with a permeability range from 10 to 1250 mD and porosity ranging from 1% to 25%. The calculated static storage resource for CO₂ in this saline system is 480 billion metric tons. However, the realistic injectivity is highly dependent on the reservoir pressure buildup, which must be considered during the CO₂ injection and postinjection for storage resource estimation and risk assessment.

EXPERIMENTAL, RESULTS, AND DISCUSSION

In the study area, there are 16 aggregated large-scale CO₂ sources (Table 1). Eight scenarios were designed to address the dynamic CO₂ storage capacity and pressure transient. To increase the injectivity and maximize the storage resource use, various strategies were explored, including injector optimization, injection rate optimization, water extraction during CO₂ injection, modifications to the ratio of vertical permeability to horizontal permeability (K_v/K_h), boundary condition plays, and relative permeability changes. Dynamic simulation was set to initiate in 2014 and end in the year 2050. Another 50-year postinjection was followed to check the pressure transient for the whole domain.

The geologic model of the basal saline system in the study area was discretized into a global grid size of 35,000 ft × 35,000 ft and a local grid refinement with cells of 7000 ft × 7000 ft (Figure 1) around the 16 CO₂ sources. The fluid model used in the modeling effort consists of brine and CO₂ that were correlated by various laws/methods for density, viscosity, and dissolution over the pressure and temperature ranges found in this geologic setting. A total of eight cases (scenarios) were designed to address CO₂ storage and pressure transient during the injection and postinjection periods (Table 2).

Table 1. Sixteen CO₂ Sources in the Study Area

Plant	State	Plant Type	Total Annual CO ₂ to be Injected (Mt)	Injection Year
Poplar River Power Station	SK	Electric generation	3.8	2022
CCRL/NEI ¹ Refinery- Upgrader Complex	SK	Petroleum and natural gas	1.7	2019
Boundary Dam Power Station	SK	Electric generation	8.6	2014, 2019
Coyote	ND	Electric generation	2.8	2021
Milton R. Young	ND	Electric generation	5.3	2019, 2024
Coal Creek	ND	Electric generation	8.9	2016, 2018
Medicine Hat û Empress	AB	Mixed	5.2	2030
Hanna	AB	Electric generation	4.4	2026
Joffe–Forestburg	AB	Petroleum and natural gas	7.1	2028
Lloydminster	AB	Electric generation	2.1	2031
Duffield – Warburg	AB	Electric generation	23.0	2019, 2021, 2023, 2025, 2027, 2029
Edmonton/Redwater	AB	Mixed	9.7	2020
Shell Quest	AB	Mixed	1.2	2015
Cold Lake–Bonnyville	AB	Petroleum and natural gas	8.3	2017
Antelope Valley/Dakota Gasification Company	ND	Multiple	8.0	2018, 2020, 2025
Leland Olds/Stanton	ND	Electric generation	4.3	2019, 2020, 2021, 2025

¹ Consumers' Cooperative Refineries Ltd./NewGrade Energy Inc.

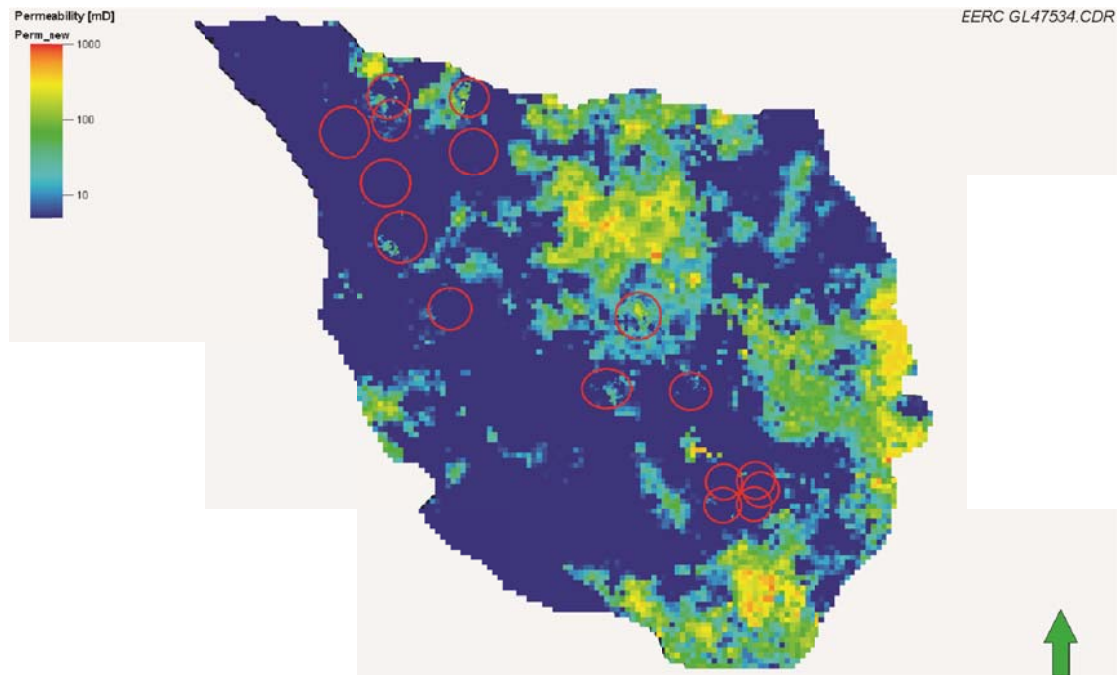


Figure 1. Global grid size 35,000 × 35,000 ft with local grid refinements in size of 7000 × 7000 ft marked by polygons overlain on the reservoir permeability.

Table 2. Eight Simulation Scenarios and Results

Case	Total Injectors	Injection to (year)	Postinjection, yr	Water Extraction Area	Kv/Kh Ratio	Real Perm. Curves	Total Injected CO ₂ , Mt
Base	16	2050	50	No	0.1	No change	82.2
1	210	2050	50	No	0.1	No change	112.3
2	210	2050	50	Duffield_Warburg	0.1	No change	183.1
3	210	2050	50	Duffield_Warburg	0.4	No change	180.0
4	210	2050	50	Duffield_Warburg	0.6	No change	179.1
5	210	2050	50	Duffield_Warburg	0.1	Changed	192.2
6	210	2064	36	Duffield_Warburg	0.1	Same as Case 5	297.6
7	210	2064	36	Duffield_Warburg	0.1	Same as Case 5	261.3

For the base case and Cases 1–5, injection was set to start in 2014, with specific “realistic” availabilities from the CO₂ sources coming online through the year 2050. Another 50-year postinjection was followed to check the pressure transients. All results are shown in Table 2. The base case includes a single injector at each of the 16 CO₂ source points (Figure 2). Results of the base case show that the total injected mass CO₂ is 82.2 Mt, which is far lower than the total CO₂ output. To improve the injectivity, 16 injectors were increased to a total of 210 wells around the various injection areas (Figure 3) in Case 1. The total mass of injected CO₂ was increased by 37% to 112.3 Mt. In Case 2, 20 water extractors were added around the injectors of the Duffield Warburg location (Figure 4). As a result of this water extraction, the total mass of injected CO₂ was increased to 183.1 Mt, 63% higher than in Case 1. Two additional cases (Cases 3 and 4) were designed to test the various ratios of vertical permeability to horizontal permeability (Kv/Kh). The cases exploring various Kv/Kh ratios showed the resulting effect on the dynamic

EERC GL49052.AI

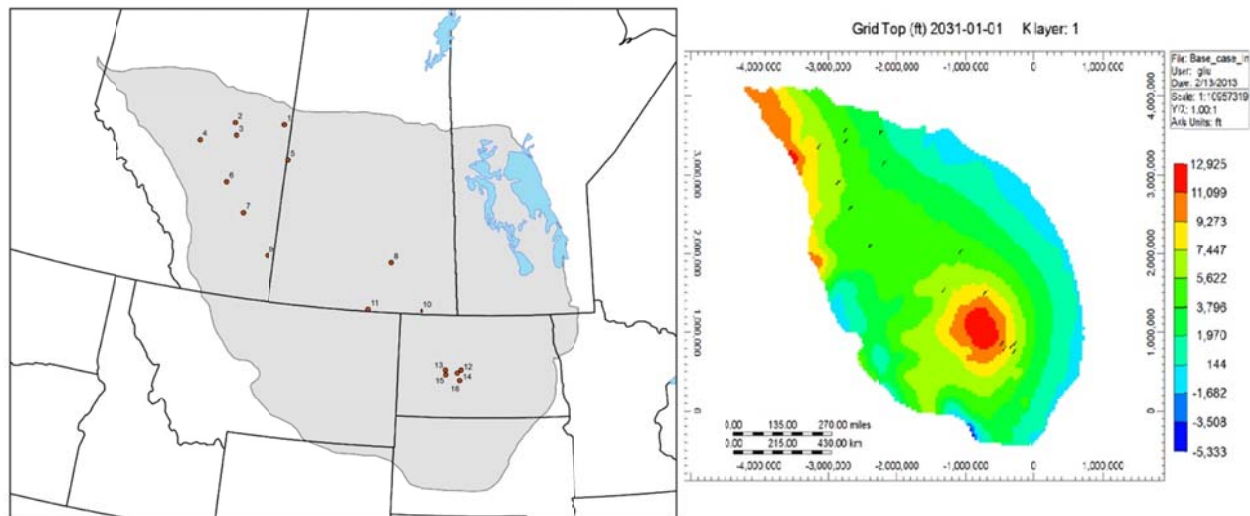


Figure 2. Location of the 16 CO₂ sources in the study area (left) and 16 injectors in the simulation model based on the location shown on the left (right).

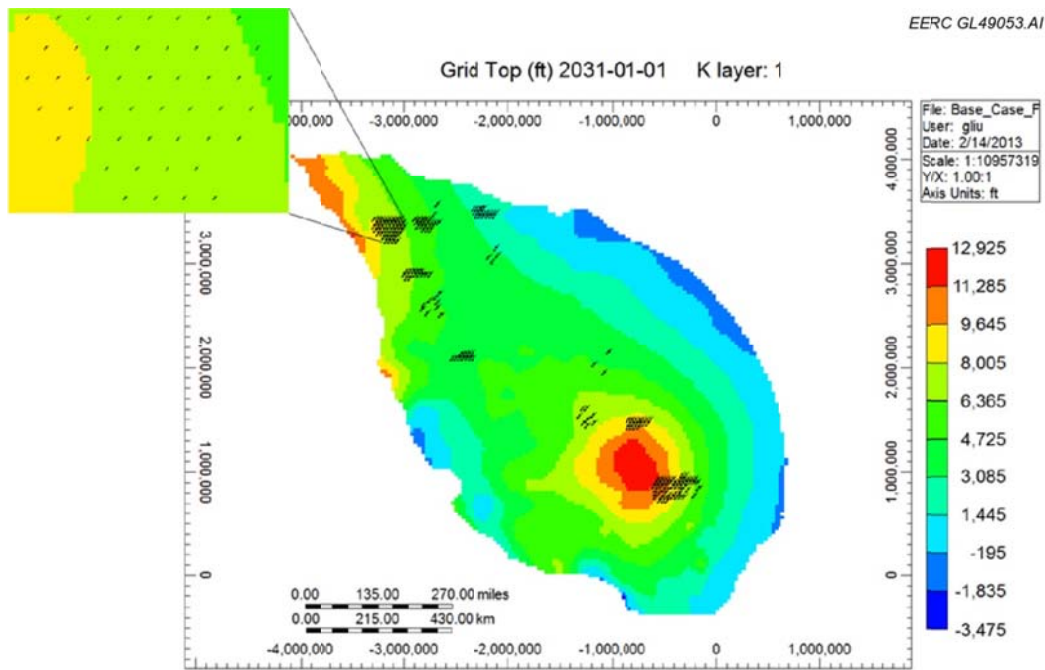


Figure 3. 210 injectors distributed among the 16 CO₂ resources.

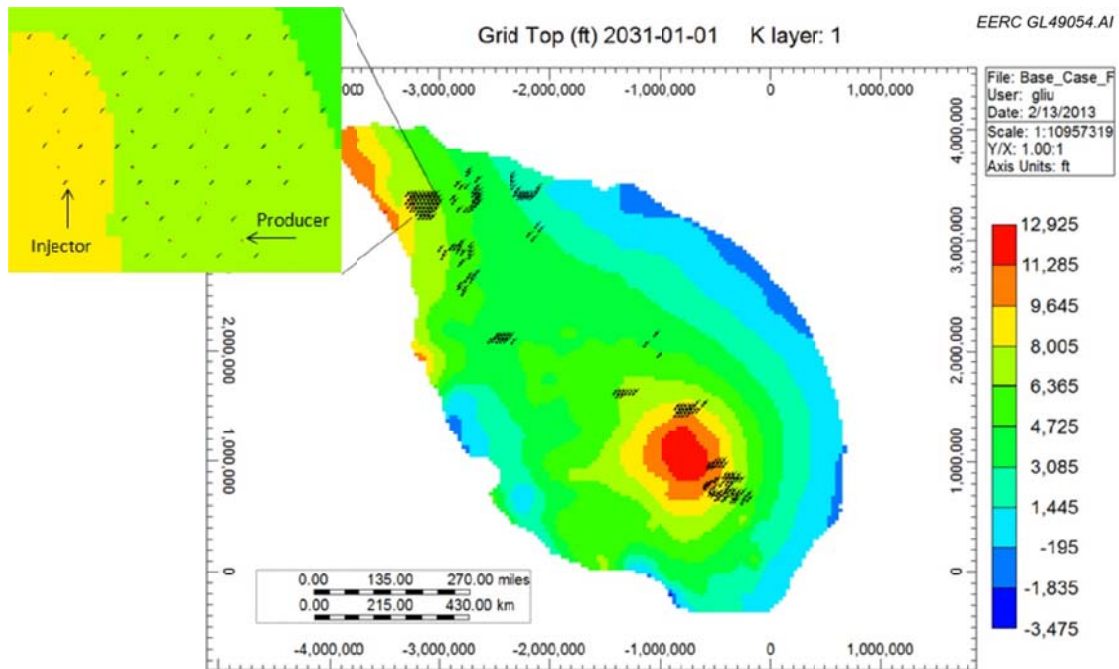


Figure 4. 20 water extractors embedded around the injectors at Duffield Warburg.

storage capacity to be very small. However, the Case 5 scenario involving changes to the relative permeability curves showed a significant increase of the storage capacity over the base case. Total mass of injected CO₂ for these various cases is shown in Figure 5.

For the scenarios investigated in Cases 6 and 7, the injection period was expanded to span 50 years and the postinjection period decreased to 36 years. The shortened postinjection period allows all cases to start and stop in the same years. In Case 6, the CO₂ injection volumes were increased to estimate how the capture of CO₂ would come online over the 50-year time span (Figure 6). In Case 7, the entire CO₂ output of the various sources was added up and injected at once (Figure 6). Both cases were simulated to the year 2064 for injection, with extra 36-year postinjection up to 2100 (Table 2, Figure 7).

The results show that the injection rate plays a significant role in CO₂ storage capacity. The higher (maximized) overall rate at the beginning results in faster reservoir pressure buildup and, ultimately, constrained the injection (Figure 6). This explains why the total injected CO₂ in Case 6 is more than the amount in Case 7. The pressure differences among initial pressure (2014), injection end pressure (2064), and 36-year postinjection pressure for Cases 6 and 7 are compared in Figures 8 and 9. Negative pressures denoted in Figures 8 and 9 are edge effects and artifacts of the modeling process.

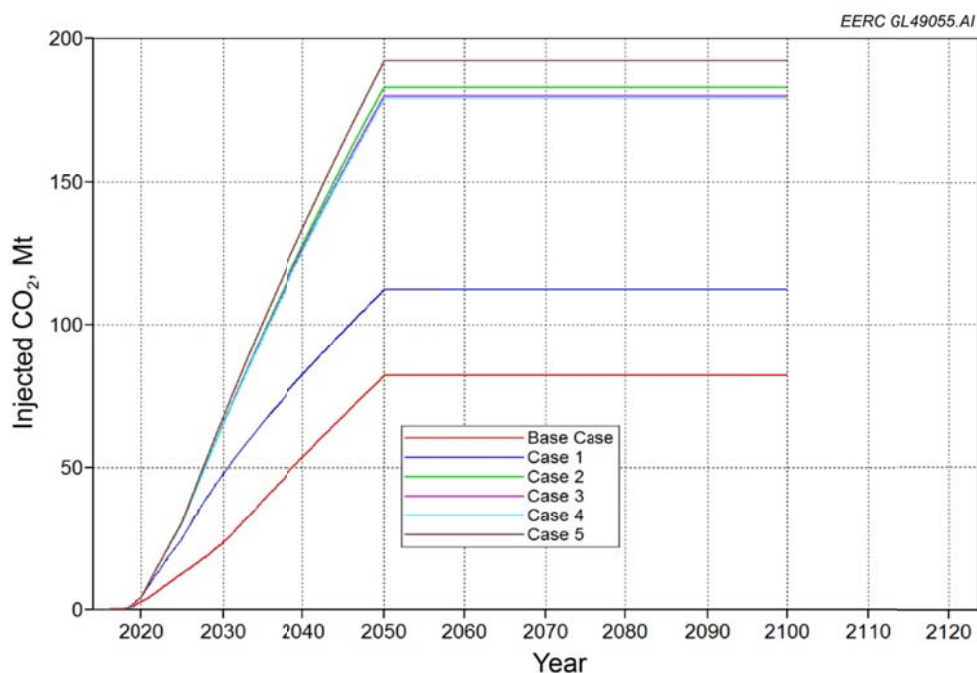


Figure 5. Total injected CO₂ with a time-stepped injection rate for Cases 1–5.

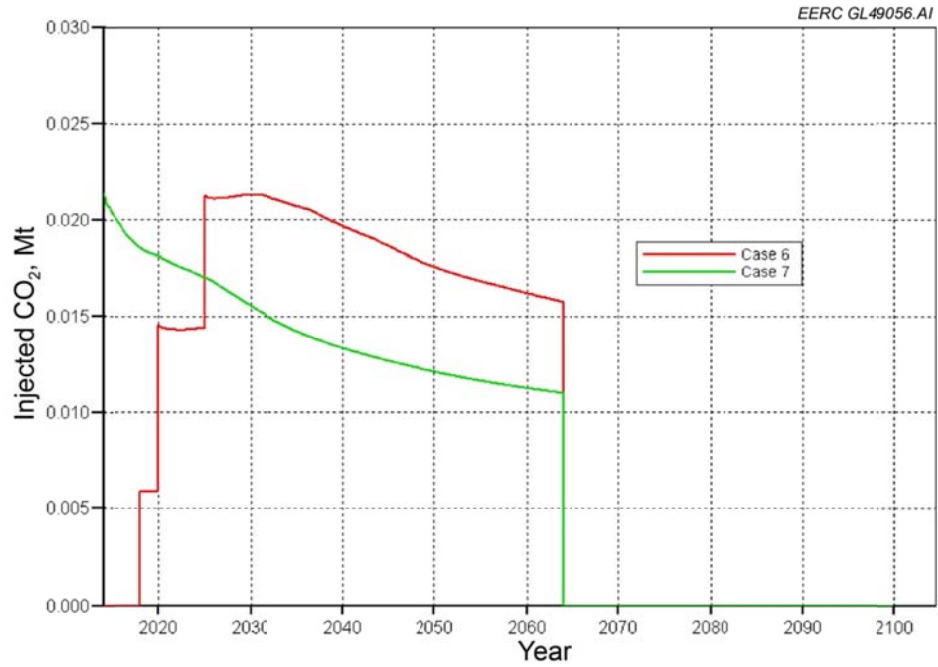


Figure 6. Injection rates for Cases 6 and 7.

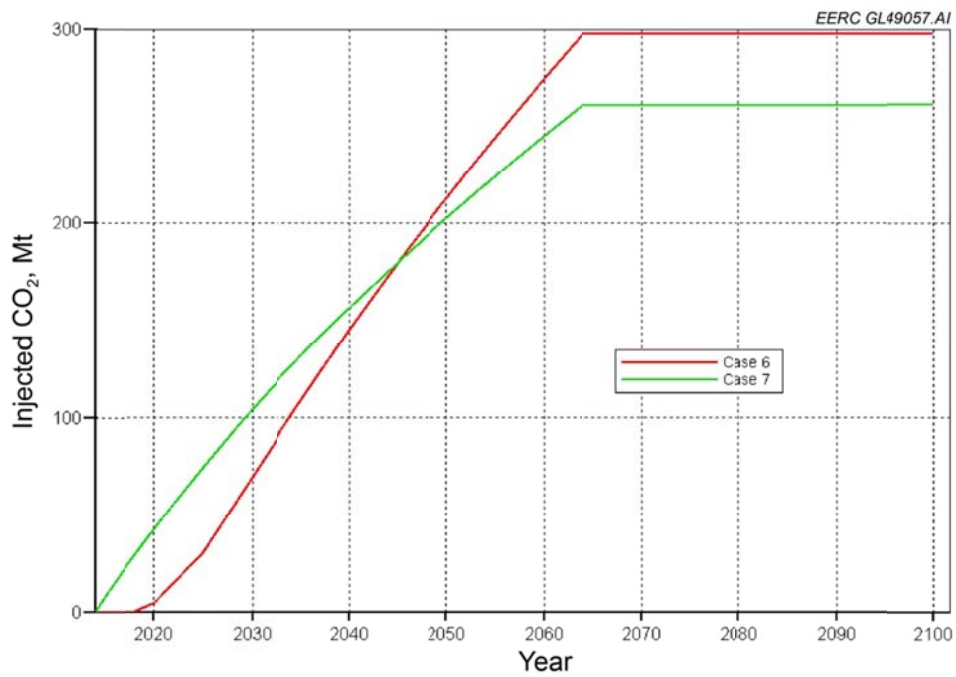


Figure 7. Total injected CO₂ for Cases 6 and 7.

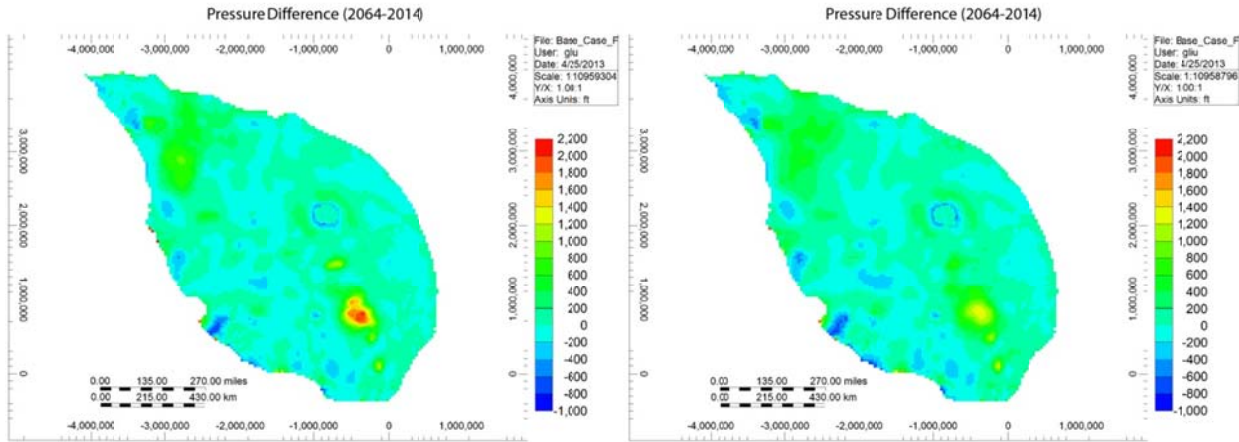


Figure 8. Case 6 pressure differences after 50-year injection (left) and after 36-year postinjection (right).

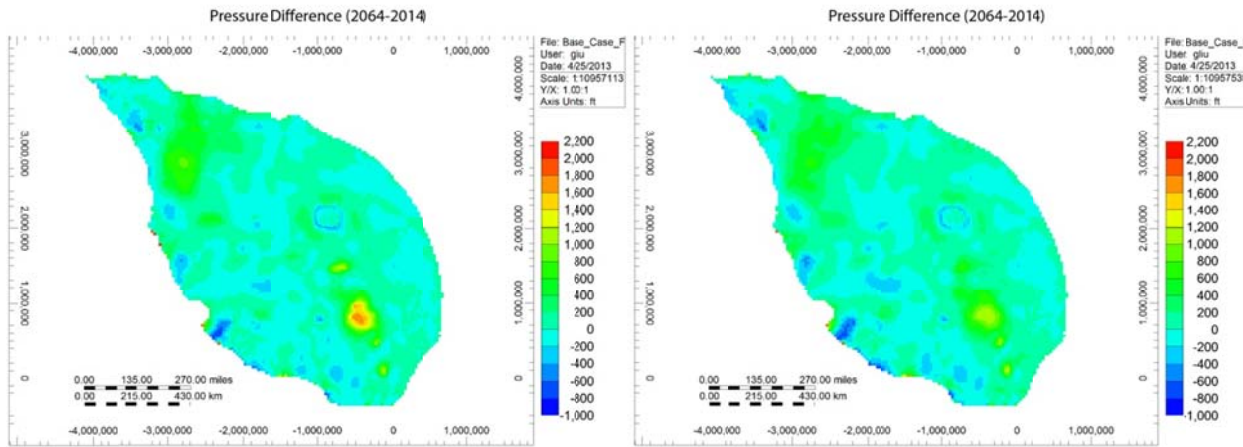


Figure 9. Case 7 pressure differences after 50-year injection (left) and after 36-year postinjection (right).

CONCLUSIONS

The base case result of one injector for each of the 16 aggregated large-scale CO₂ sources show that the injectivity of the system is not sufficient to accommodate the cumulative mass of emitted CO₂. Exploring various optimization strategies, such as increasing the number of injectors, adding water extractors around the injectors, and modifying the relative permeability, showed a moderate to significant role in increasing the injectivity and, ultimately, the total amount of injected CO₂. The best case of the various scenarios is 3.17 times higher than the base case. However, even with this increased injectivity, the system was not able to accommodate the cumulative mass of CO₂ over the given time frame. It should be noted that all of the simulation efforts in this report are based on one geological realization. This single realization likely does

not reflect the true natural characteristics of the injection zones at a particular CO₂ source location. As the next step in optimizing the potential storage resource, the aggregated CO₂ sources will be separated into 25 source points. Each of these new source points will be shifted geographically to coincide with the more promising geologic properties as depicted by the geologic model. In addition, more injection wells will be modeled at each of these new locations.

The successful exploration of the study for CO₂ storage in the basal saline system of central North America provides a basic guideline to address evaluations of large-scale CO₂ storage demonstration projects. Specifically, the efforts help to answer questions regarding reservoir pressure buildup over the injection and postinjection periods and track the CO₂ movement. These play a crucial role in the whole process of CO₂ monitoring, verification, and accounting for such a large-scale case of CO₂ storage estimation.